

Article

Interval-Type 3 Fuzzy Differential Evolution for Designing an Interval-Type 3 Fuzzy Controller of a Unicycle Mobile Robot

Cinthia Peraza ¹, Patricia Ochoa ¹, Oscar Castillo ¹ and Zong Woo Geem ^{2,*}¹ Tijuana Institute of Technology, TecNM, Tijuana 22379, Mexico² College of IT Convergence, Gachon University, Seongnam 13120, Korea

* Correspondence: geem@gachon.ac.kr

Abstract: Recently, interval-type 3 fuzzy systems have begun to appear in different research areas. This article outlines a methodology for the parameterization of interval type-3 membership functions using vertical cuts applied to the dynamic parameter adaptation of the differential evolution algorithm and implemented in an interval-type 3 Sugeno controller. This methodology was applied to the dynamic adaptation of the F (mutation) parameter in differential evolution to improve the performance of this method as the generations occur. To test the type-3 fuzzy differential evolution algorithm, the optimal design of a type-3 Sugeno controller was considered. In this case, the parameterization of the type-3 membership functions of this Sugeno fuzzy controller was performed. The experimentation is based on the application of three different noise levels for validation of the efficacy of the method and performing a comparison study with respect to other articles in the literature. The main idea is to implement the parameterization of interval type-3 membership functions to enhance the ability of differential evolution in designing an optimal interval type-3 system to control a unicycle mobile robot.

Keywords: interval type-3 fuzzy logic; differential evolution; fuzzy controller**MSC:** 03B52; 03E72; 62P30

Citation: Peraza, C.; Ochoa, P.; Castillo, O.; Geem, Z.W. Interval-Type 3 Fuzzy Differential Evolution for Designing an Interval-Type 3 Fuzzy Controller of a Unicycle Mobile Robot. *Mathematics* **2022**, *10*, 3533. <https://doi.org/10.3390/math10193533>

Academic Editor: Krystian Jobczyk

Received: 2 September 2022

Accepted: 24 September 2022

Published: 28 September 2022

Publisher's Note: MDPI stays neutral with regard to jurisdictional claims in published maps and institutional affiliations.



Copyright: © 2022 by the authors. Licensee MDPI, Basel, Switzerland. This article is an open access article distributed under the terms and conditions of the Creative Commons Attribution (CC BY) license (<https://creativecommons.org/licenses/by/4.0/>).

1. Introduction

In today's world, the need for solving complex and iterative tasks has grown exponentially. Artificial intelligent techniques help solve complex problems and reduce the time to perform certain tasks in many areas, as can be seen in the following machine learning and deep learning applications [1–4].

The general concepts of the fuzzy logic theory presented by Zadeh [5] have evolved over the years, in order to adapt and improve the solutions to tasks that are required in today's world. Fuzzy logic has evolved as follows, type-1 (T1-FSs), interval type-2 (IT2-FSs), generalized type-2 (GT2-FSs), intuitionistic type-2 (T2-IFSs) and shadowed type-2 (ST2-FSs) until arriving at interval type-3 fuzzy systems (IT3-FSs), and in the future, we could have type-n fuzzy systems. These are very popular techniques that have been utilized to deal with problems with high levels of complexity, due to their capability in handling uncertainty.

Fuzzy logic can be adapted for solving many problems in real life, and in the following articles, the application of fuzzy logic has been utilized for the dynamic adaptation of parameters in various algorithms applied to different benchmark problems with T1-FSs [6,7], IT2-FSs [8,9], GT2-FSs [10,11], ST2-FSs [12,13] and intuitionistic fuzzy systems (T2-IFSs) [14,15].

Interval type-3 is a relatively new theory for modeling systems with greater uncertainty. Currently, there are ongoing research works in different areas of the literature, the most recent of which is used for the creation of fuzzy systems in this work, is a methodology for building IT3-FSs based on the justifiable granularity concept [16]. Despite being a

very recent topic, there are multiple works that have already been carried out utilizing IT3-FSSs [17–22]. The main objective was to implement the parameterization of interval type-3 membership functions to improve the performance of the differential evolution (DE) algorithm and to implement an IT3-FSSs to control a unicycle mobile robot. We note that in the review of the existing literature, there are no published works on type-3 fuzzy applied in parameter adaptation for the DE algorithm, which indicates a research gap in the existing state of the art. In addition, there have not been any papers on the application of the DE algorithm for optimizing interval type-3 Sugeno controllers, which is another gap in the state of the art. In this sense, this work addresses these two research gaps in the literature. Accordingly, the main contributions are stated in the following paragraph.

The main contributions are stated as follows. A novel parameter adaptation approach for the DE algorithm is proposed by utilizing the parameterization of interval type-3 membership functions using vertical cuts with the goal of managing in a better fashion the uncertainty of the parameter setting problem in the DE algorithm, for achieving better results in accuracy and performance. The proposed type-3 fuzzy DE algorithm (IT3FDE) approach was applied to the problem of finding optimal Sugeno type-3 fuzzy controllers for mobile robots, which was not previously done in the literature. An extensive comparison of results demonstrates that type-3 fuzzy helps improve the results of the DE algorithm and also the obtained type-3 controllers perform better when used in controlling the mobile robots.

The order of the sections is given as: Section 2 offers the interval type-3 fuzzy logic theory, Section 3 summarizes the theory of the DE algorithm, Section 4 presents the proposed methodology for the DE algorithm and the case study for the application, Section 5 summarizes results and Section 6 outlines conclusions.

2. Materials and Methods

The new type-3 fuzzy set (IT3-FSSs) [23,24], represented by $A^{(3)}$, can be expressed by a function, called membership function (MF) of $A^{(3)}$, in the Cartesian product $X \times [0, 1] \times [0, 1]$ in $[0, 1]$, where X is the universe of $A^{(3)}$, x . The MF of $\mu_{A^{(3)}}$ is expressed by $\mu_{A^{(3)}}(x, u, v)$ and is known as a type-3 MF (T3 MF) of IT3-FSSs. The mathematical form is expressed in Equations (1)–(7).

$$\mu_{A^{(3)}} : X \times [0, 1] \times [0, 1] \rightarrow [0, 1] \tag{1}$$

$$A^{(3)} = \{(x, u(x), v(x, u), \mu_{A^{(3)}}(x, u, v) \mid x \in X, u \in U \subseteq [0, 1], v \in V \subseteq [0, 1]\} \tag{2}$$

$$A^{(3)} = \int_{x \in X} \int_{u \in [0, 1]} \int_{v \in [0, 1]} \mu_{A^{(3)}}(x, u, v) / (x, u, v) \tag{3}$$

$$A^{(3)} = \int_{x \in X} \left[\int_{u \in [0, 1]} \left[\int_{v \in [0, 1]} \mu_{A^{(3)}}(x, u, v) / v \right] / u \right] / x \tag{4}$$

$$A^{(3)} = \int_{x \in X} \mu_{A_x^{(3)}}(u, v) / x \tag{5}$$

$$\mu_{A_x^{(3)}}(u, v) = \int_{u \in [0, 1]} \mu_{A_{(x,u)}^{(3)}}(v) / u \tag{6}$$

$$\mu_{A_x^{(3)}}(v) = \int_{v \in [0, 1]} \mu_{A^{(3)}}(x, u, v) / v \tag{7}$$

If $\mu_{A^{(3)}}(x, u, v) = 1$, the IT3-FSSs, $A^{(3)}$, is simplified to an interval type-3 fuzzy set (IT3-FSSs) symbolized by \mathbb{A} , formulated by (8).

$$\mathbb{A} = \int_{x \in X} \left[\int_{u \in [0, 1]} \left[\int_{v \in [\underline{\mu}_{\mathbb{A}}(x, u), \bar{\mu}_{\mathbb{A}}(x, u)]} 1 / v \right] / u \right] / x \tag{8}$$

where Equation (8) is defined by Equations (9)–(11):

$$\mu_{\mathbb{A}(x,u)}(v) = \int_{v \in [\underline{\mu}_{\mathbb{A}}(x,u), \bar{\mu}_{\mathbb{A}}(x,u)]} 1/v \tag{9}$$

$$\mu_{\mathbb{A}(x,u)}(v) = \int_{u \in [0,1]} \left[\int_{v \in [\underline{\mu}_{\mathbb{A}}(x,u), \bar{\mu}_{\mathbb{A}}(x,u)]} 1/v \right] / u \tag{10}$$

$$\mathbb{A} = \int_{x \in X} \mu_{\mathbb{A}(x)}(u, v) / x \tag{11}$$

Equation (8) can be simplified as an interval type-3 membership function (T3 MF), $\tilde{\mu}_{\mathbb{A}}(x, u) \in [\underline{\mu}_{\mathbb{A}}(x, u), \bar{\mu}_{\mathbb{A}}(x, u)]$, expressed in Equation (12).

$$\mathbb{A} = \int_{x \in X} \int_{u \in [0,1]} \tilde{\mu}_{\mathbb{A}}(x, u) / (x, u) \tag{12}$$

where the lower interval type-2 membership function (T2 MF) $\underline{\mu}_{\mathbb{A}}(x, u)$ is a subset in the upper T2 MF $\bar{\mu}_{\mathbb{A}}(x, u)$, this is, $\underline{\mu}_{\mathbb{A}}(x, u) \subseteq \bar{\mu}_{\mathbb{A}}(x, u)$, then $\underline{\mu}_{\mathbb{A}}(x, u) \leq \bar{\mu}_{\mathbb{A}}(x, u)$, and can be concluded that an IT3-FSSs is formulated by two IT2-FSSs, one inferior $\underline{\mathbb{A}}$ with $\underline{\mu}_{\mathbb{A}}(x, u)$, and another superior $\bar{\mathbb{A}}$, with $\bar{\mu}_{\mathbb{A}}(x, u)$ formulated by Equations (13) and (14):

$$\underline{\mathbb{A}} = \int_{x \in X} \int_{u \in [0,1]} \underline{\mu}_{\mathbb{A}}(x, u) / (x, u) = \int_{x \in X} \left[\int_{u \in [0,1]} \underline{f}_x(u) / u \right] / x \tag{13}$$

$$\bar{\mathbb{A}} = \int_{x \in X} \int_{u \in [0,1]} \bar{\mu}_{\mathbb{A}}(x, u) / (x, u) = \int_{x \in X} \left[\int_{u \in [0,1]} \bar{f}_x(u) / u \right] / x \tag{14}$$

where the secondary MFs of $\underline{\mathbb{A}}$ and $\bar{\mathbb{A}}$ are type-1 membership function (T1-MFs) formulated by Equations (15) and (16):

$$\mu_{\underline{\mathbb{A}}(x)}(u) = \int_{u \in J_x} \underline{f}_x(u) / u \tag{15}$$

$$\mu_{\bar{\mathbb{A}}(x)}(u) = \int_{u \in J_x} \bar{f}_x(u) / u \tag{16}$$

To represent the T3 MF from IT3-FSSs, \mathbb{A} , is a surface, $\tilde{\mu}_{\mathbb{A}}(x, u)$ because of the union of vertical-slices in x , where each vertical cut in $x = x'$ is an embedded secondary T2 MF, $\tilde{f}_{x'}(u)$, in other words, $\tilde{f}_{x'}(u) \in 1 / [\underline{\mu}_{\mathbb{A}}(x', u), \bar{\mu}_{\mathbb{A}}(x', u)]$ or $\tilde{f}_{x'}(u) \in [\underline{f}_{x'}(u), \bar{f}_{x'}(u)]$. Therefore, Equation (12) can be simplified to Equation (17), we can see Figure 1.

$$\mathbb{A} = \int_{x \in X} \int_{u \in [0,1]} \tilde{\mu}_{\mathbb{A}}(x, u) / (x, u) = \int_{x \in X} \left[\int_{u \in [0,1]} \tilde{f}_x(u) / u \right] / x \tag{17}$$

where $\tilde{\mu}_{\mathbb{A}}(x, u) \in [\underline{\mu}_{\mathbb{A}}(x, u), \bar{\mu}_{\mathbb{A}}(x, u)]$ Equation (17) can be reformulated as Equations (18) and (19).

$$\mathbb{A} = \int_{x \in X} \mu_{\mathbb{A}(x)}(u) / x = \int_{x \in X} \left[\int_{u \in [0,1]} \tilde{f}_x(u) / u \right] / x \tag{18}$$

where $\mu_{\mathbb{A}(x)}(u)$ is an interval type-2 fuzzy set (IT2-FSSs), formulated by Equation (19).

$$\mu_{\mathbb{A}(x)}(u) = \int_{u \in J_x} \tilde{f}_x(u) / u = \int_{u \in [\underline{f}_x(u), \bar{f}_x(u)]} 1 / u \tag{19}$$

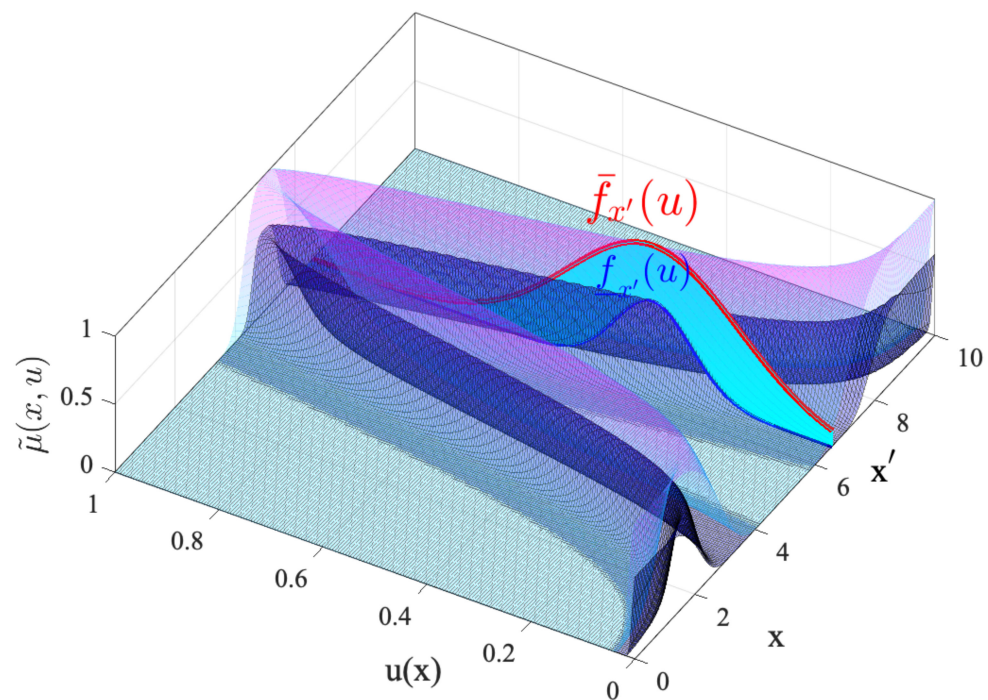


Figure 1. IT3-FSs,, with T3 MF, and an embedded vertical cut, with the footprint of uncertainty (FOU) in sky blue color.

3. Differential Evolution Algorithm

The DE algorithm has had numerous applications for quite some time; DE is an algorithm that is currently used in different disciplines, to mention a few recently: minimization of agency and user costs, optimization of the duration of traffic interruption and environmental impact [25], the performance of solar systems depending on the precise modeling of the cell parameters [26], the customer scheduling problem to minimize the total completion time [27], as well adaptations to the algorithm have been made, which have proven to have good results [28–31].

The use of the DE algorithm is one of the main characteristics of this work in its original form, the mathematical structure of the algorithm is shown below, which is described in Equations (20)–(29).

Population structure (NP)

$$P_{x,g} = (x_{i,g}), i = 0, 1, 2, \dots, Np - 1, g = 0, 1, 2, \dots, g_{max}, \tag{20}$$

$$x_{i,g} = (x_{j,i,g}), j = 0, 1, 2, \dots, D - 1 \tag{21}$$

$$P_{v,g} = (v_{i,g}), i = 0, 1, 2, \dots, Np - 1, g = 0, 1, 2, \dots, g_{max}, \tag{22}$$

$$v_{i,g} = (v_{j,i,g}), j = 0, 1, 2, \dots, D - 1 \tag{23}$$

$$P_{u,g} = (u_{i,g}), i = 0, 1, 2, \dots, Np - 1, g = 0, 1, 2, \dots, g_{max}, \tag{24}$$

$$u_{i,g} = (u_{j,i,g}), j = 0, 1, 2, \dots, D - 1 \tag{25}$$

Initialization

$$x_{j,i,0} = rand_j(0, 1) \cdot (b_{j,U} - b_{j,L}) + b_{j,L} \tag{26}$$

Mutation (F)

$$v_{i,g} = x_{r_0,g} + F \cdot (x_{r_1,g} - x_{r_2,g}) \tag{27}$$

Crossover (CR)

$$u_{i,g} = u_{j,i,g} \{ v_{j,i,g} \text{ if } (rand_j(0, 1) \leq Cr \text{ or } j = j_{rand}) x_{j,i,g} \text{ otherwise} \} \tag{28}$$

Selection

$$x_{i,g+1} = \begin{cases} u_{i,g} & \text{if } f(u_{i,g}) \leq f(x_{i,g}) \\ x_{i,g} & \text{otherwise} \end{cases} \quad (29)$$

4. Methodology

This section is structured into two parts; in the first, an overview of the model approach suggested in the proposal for the parameterization of interval type-3 membership functions using vertical cuts for the dynamic adaptation of the F parameter in the DE algorithm is shown and in the second part, a general view of the implementation of the parameterization of the membership functions using vertical cuts for the interval type-3 Sugeno controller.

4.1. Proposed Method

The fuzzy system used in this experimentation is interval type-3, which we will call for this work IT3FDE and has the following characteristics:

It has an input representing the Generations and an output F that corresponds to the mutation parameter in the IT3FDE algorithm. The system is of type Mamdani, both input and the output are composed of three T3 MF and contain three rules.

The representation of the system can be seen in Figure 2, which contains the description mentioned in the previous paragraph, while Figure 3 shows the surface obtained with the combination of rules utilized in the system, and in Table 1, the set of rules is listed.

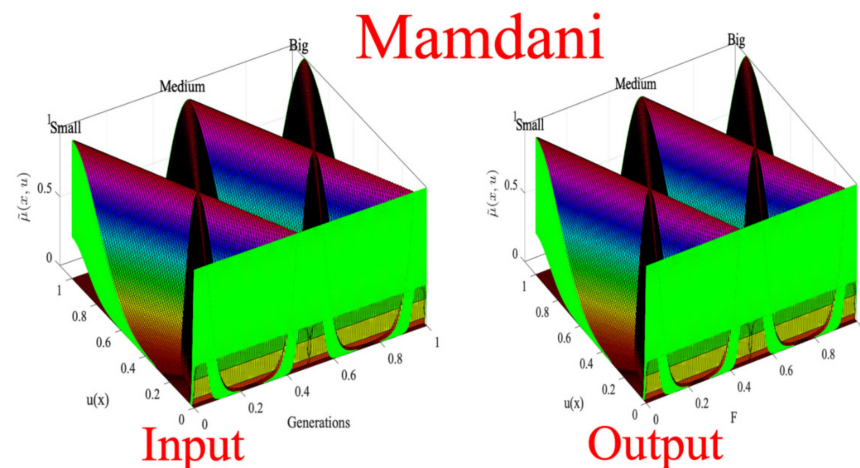


Figure 2. Differential evolution algorithm with interval type-3 fuzzy set (IT3FDE).

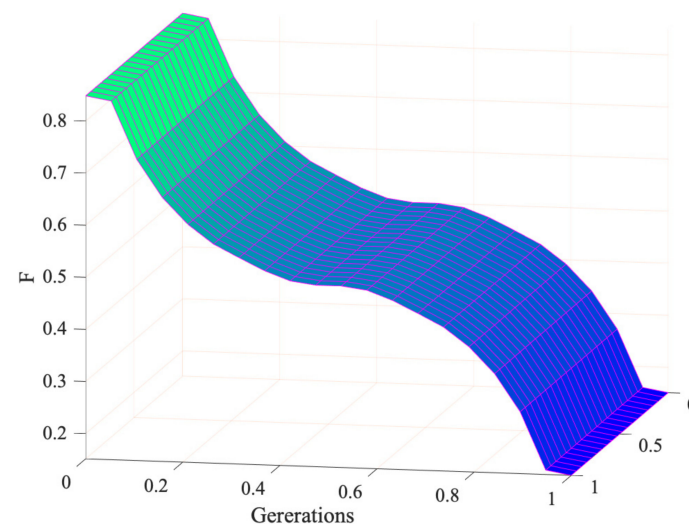


Figure 3. The surface of the IT3FDE system.

Table 1. Rules of the IT3FDE system.

| F Generation | Small | Medium | Big |
|--------------|-------|--------|-------|
| Small | - | - | Small |
| Medium | - | Medium | - |
| Big | Big | - | - |

The membership function by which the fuzzy system is composed is ScaleTriScaleGaussT3MF, the visual representation of the MF is presented in Figure 4 and its mathematical representation is expressed in Equation (30).

$$\tilde{\mu}_{\mathbb{A}}(x, u) = \text{ScaleTriScaleGaussT3MF}(x, \{[a_1, b_1, c_1]\}, \lambda, [\ell_1, \ell_2]) \tag{30}$$

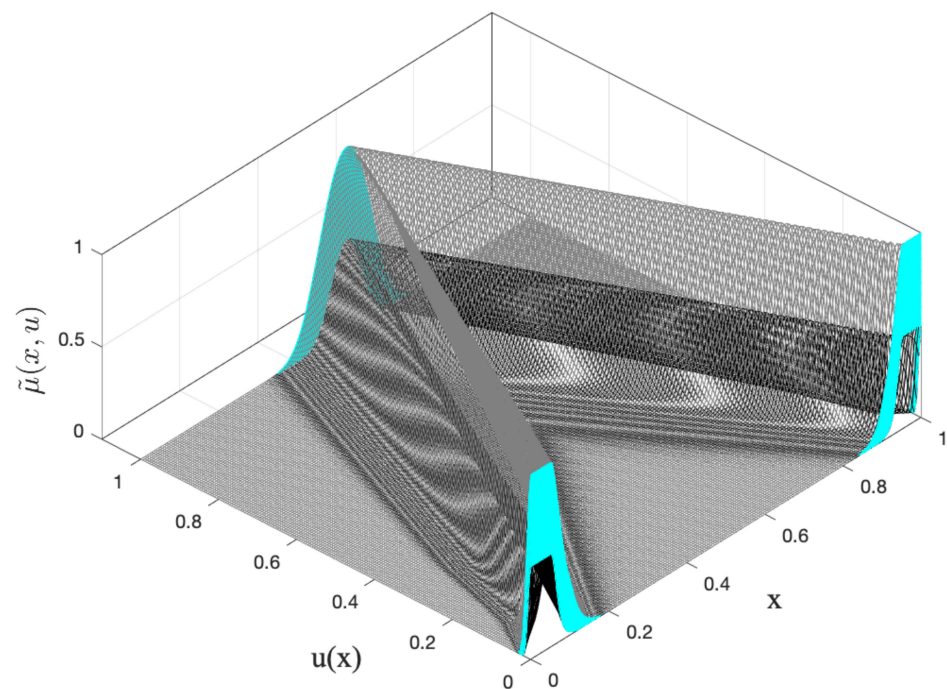


Figure 4. ScaleTriScaleGaussT3MF used in the IT3FDE.

The interval type-3 triangular membership function, $\tilde{\mu}_{\mathbb{A}}(x, u) = \text{ScaleTriScaleGaussT3MF}$, with triangular $FOU(\mathbb{A})$, is characterized with parameters $[a_1, b_1, c_1]$ (UpperParameters) for upper membership function (UMF) and λ (LowerScale), ℓ (LowerLag) parameters for lower membership function (LMF), to form the domain of uncertainty (DOU) with parameters $DOU = [\underline{\mu}(x), \overline{\mu}(x)]$. The vertical slices $\mathbb{A}_{(x)}(u)$ characterize the $FOU(\mathbb{A})$, these are IT2-FSs with Gaussian T2 MF, $\mu_{\mathbb{A}(x)}(u)$ with parameters $[\sigma_u, m(x)]$ for the UMF and LMF λ (LowerScale), λ (LowerLag). The $\tilde{\mu}_{\mathbb{A}}(x, u) = \text{ScaleTriScaleGaussT3MF}(x, \{[a_1, b_1, c_1]\}, \lambda, [\ell_1, \ell_2])$ is described by the following Equations (31) and (32):

$$\overline{\mu}(x) = \begin{cases} 0 & x < a_1 \\ \frac{x-a_1}{b_1-a_1} & a_1 \leq x \leq b_1 \\ \frac{c_1-x}{c_1-b_1} & b_1 < x \leq c_1 \\ 0 & x > c_1 \end{cases} \tag{31}$$

$$\begin{aligned}
 a_2 &= b_1 - (b_1 - a_1)(1 - \ell_1) \\
 c_2 &= b_1 + (c_1 - b_1)(1 - \ell_2) \\
 \mu(x) &= \begin{cases} 0 & x < a_2 \\ \frac{x-a_2}{b_1-a_2} & a_2 \leq x \leq b_1 \\ \frac{c_2-x}{c_2-b_1} & b_1 < x \leq c_2 \\ 0 & x > c_2 \end{cases} \tag{32}
 \end{aligned}$$

The function $\mu(x)$ is multiplied by the parameter λ to form the LMF of the DOU, $\underline{\mu}(x)$, described as: $\underline{\mu}(x) = \lambda \mu(x)$. Then, $\bar{u}(x)$ and $\underline{u}(x)$ are the upper and lower DOU limits. The range, $\delta(\bar{u})$ and radius, σ_u of the FOU are defined in Equations (33) and (34):

$$\begin{aligned}
 \delta(u) &= \bar{u}(x) - \underline{u}(x) \\
 \sigma_u &= \frac{\delta(u)}{2\sqrt{3}} + \varepsilon \tag{33}
 \end{aligned}$$

The apex or core, $m(x)$, of the T3 MF $\tilde{\mu}(x, u)$, is defined by Equations:

$$m(x) = \begin{cases} 0 & x < a \\ \frac{x-a}{b_1-a} & a \leq x \leq b_1 \\ \frac{c-x}{c-b_1} & b_1 < x \leq c \\ 0 & x > c \end{cases} \tag{34}$$

where $a = (a_1 + a_2)/2$ and $c = (c_1 + c_2)/2$. Then, vertical cuts with T2 MF $\mu_{\mathbb{A}(x)}(u) = [\underline{\mu}_{\mathbb{A}(x)}(u), \bar{\mu}_{\mathbb{A}(x)}(u)]$. They are described by the following Equations (35) and (36):

$$\bar{\mu}_{\mathbb{A}(x)}(u) = \exp\left[-\frac{1}{2}\left(\frac{u - m(x)}{\sigma_u}\right)^2\right] \tag{35}$$

$$\underline{\mu}_{\mathbb{A}(x)}(u) = \lambda \cdot \exp\left[-\frac{1}{2}\left(\frac{x - m(x)}{\sigma_u^*}\right)^2\right] \tag{36}$$

where $\sigma_u^* = \sigma_u \sqrt{\frac{\ln(\ell)}{\ln(\varepsilon)}}$ and $\ell = (\ell_1 + \ell_2)/2$. Supposing $\ell = 0$ then $\sigma_u^* = \sigma_u$.

Accordingly, $\bar{\mu}_{\mathbb{A}(x)}(u)$ and $\underline{\mu}_{\mathbb{A}(x)}(u)$ are the UMF and LMF of the IT2-FSs of the vertical cuts.

4.2. Mobile Robot System

The main task of a mobile robot is the search for a succession of positions, in this case of a unicycle mobile robot, whose objective is to take it from an initial to a final state. The elements of the mobile robot system can be found in Figure 5. Kinematic knowledge of robot operation is present in [32].

This control case has been used in other works as we can see in [33–36]. The main difference with the existing articles in the literature is that in this work, the theory of IT3-FS was implemented to achieve the control of a mobile robot system.

The interval type-3 membership functions (T3 MF) that were implemented in the IT3-FS mobile robot are the interval type-3 triangular (ScaleTriScaleGauss) and the interval type-3 trapezoidal (ScaleTrapScaleGauss). The mathematical operations for the construction of the ScaleTriScaleGauss function are shown in Equations (31)–(36) and the ScaleTrapScaleGauss in Equations (36)–(41).

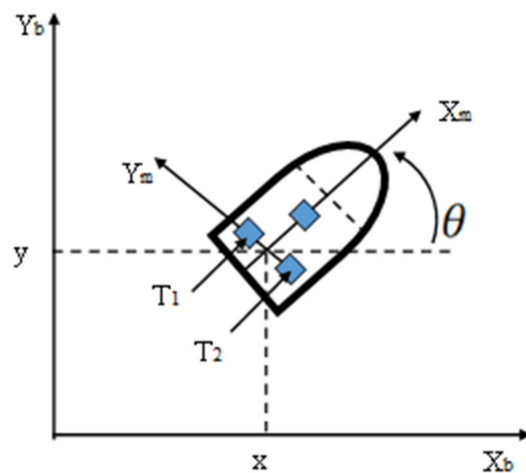


Figure 5. Diagram of the mobile robot system.

The interval type-3 trapezoidal MF, $\tilde{\mu}_{\mathbb{A}}(x, u) = \text{ScaleTrapScaleGaussT3MF}$ with triangular $FOU(\mathbb{A})$, is characterized with parameters $[a_1, b_1, c_1, d_1]$ (UpperParameter) for UMF and parameters λ (LowerScale), ℓ (LowerLag) for LMF to form the $DOU = [\underline{\mu}(x), \bar{\mu}(x)]$. The vertical slices $\mathbb{A}_{(x)}(u)$ characterize the $FOU(\mathbb{A})$, these are IT2-FSs with interval type-2 Gaussians membership functions (T2 MF), $\mu_{\mathbb{A}(x)}(u)$ with parameters $[\sigma_u, m(x)]$ for UMF and LMF λ (LowerScale), ℓ (LowerLag). The T3 MF $\tilde{\mu}_{\mathbb{A}}(x, u) = \text{ScaleTrapScaleGaussT3MF}(x, \{[a_1, b_1, c_1, d_1]\}, \lambda, [\ell_1, \ell_2])$ is described by the following Equation (37).

$$\bar{\mu}(x) = \begin{cases} 0 & x < a_1 \\ \frac{x-a_1}{b_1-a_1} & a_1 \leq x \leq b_1 \\ 1 & b_1 < x \leq c_1 \\ \frac{d_1-x}{d_1-c_1} & c_1 < x \leq d_1 \\ 0 & x > d_1 \end{cases} \tag{37}$$

The LMF of the DOU, $\underline{\mu}(x)$, is defined by the values (a_2, b_2, c_2, d_2) , where these depend on the parameters (a_1, b_1, c_1, d_1) of the UMF of the DOU, $\bar{\mu}(x)$, and the elements of the vector lowerLag(ℓ), as seen in Equation (38).

$$\begin{aligned} \Delta r &= (b_1 - a_1) \ell_1 \\ \Delta l &= (d_1 - c_1) \ell_2 \\ a_2 &= a_1 + \Delta r, \quad b_2 = b_1 + \Delta r, \quad c_2 = c_1 - \Delta l, \quad d_2 = d_1 - \Delta l \end{aligned}$$

$$\underline{\mu}(x) = \begin{cases} 0 & x < a_2 \\ \frac{x-a_2}{b_2-a_2} & a_2 \leq x \leq b_2 \\ 1 & b_2 < x \leq c_2 \\ \frac{d_2-x}{d_2-c_2} & c_2 < x \leq d_2 \\ 0 & x > d_2 \end{cases} \tag{38}$$

To form the upper and lower DOU limits is presented in Equation (33). The apex or center, $m(x)$, of the T3 MF $\tilde{\mu}(x, u)$, is defined by Equation (39).

$$m(x) = \begin{cases} 0 & x < a \\ \frac{x-a}{b-a} & a \leq x < b \\ 1 & b \leq x \leq c \\ \frac{d-x}{d-c} & c < x \leq d \\ 0 & x > d \end{cases} \tag{39}$$

where $a = (a_1 + a_2)/2$, $b = (b_1 + b_2)/2$, $c = (c_1 + c_2)/2$ and $d = (d_1 + d_2)/2$. Then, the vertical slices with IT2MF, $\mu_{\Delta(x)}(u) = [\underline{\mu}_{\Delta(x)}(u), \bar{\mu}_{\Delta(x)}(u)]$, are described by Equations (35) and (36).

After analyzing the mathematical knowledge of this system, the implementation of a Sugeno interval type-3 mobile robot fuzzy system (IT3FC) was carried out. The system consists of two antecedents which are Linear Velocity Error (LVE), Angular Velocity Error (WVE) and two consequents with Sugeno coefficients to control the right wheel (Torque 1) and the left wheel (Torque 2). Figures 6 and 7 show the architecture of the T3 MF of the antecedents and consequents of the IT3-FSs. The linguistic variables used are Negative (Neg), Zero and Positive (Pos).

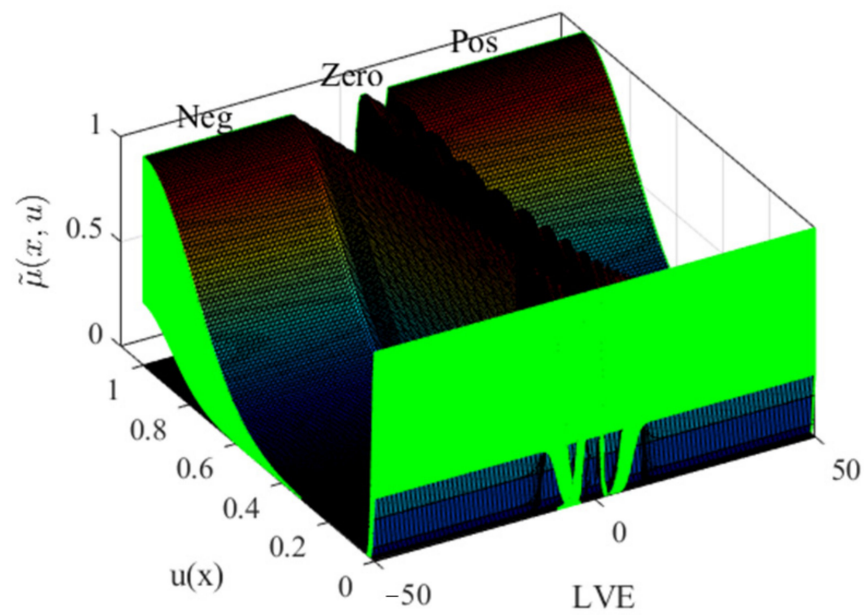


Figure 6. The architecture of the antecedent membership function (LVE).

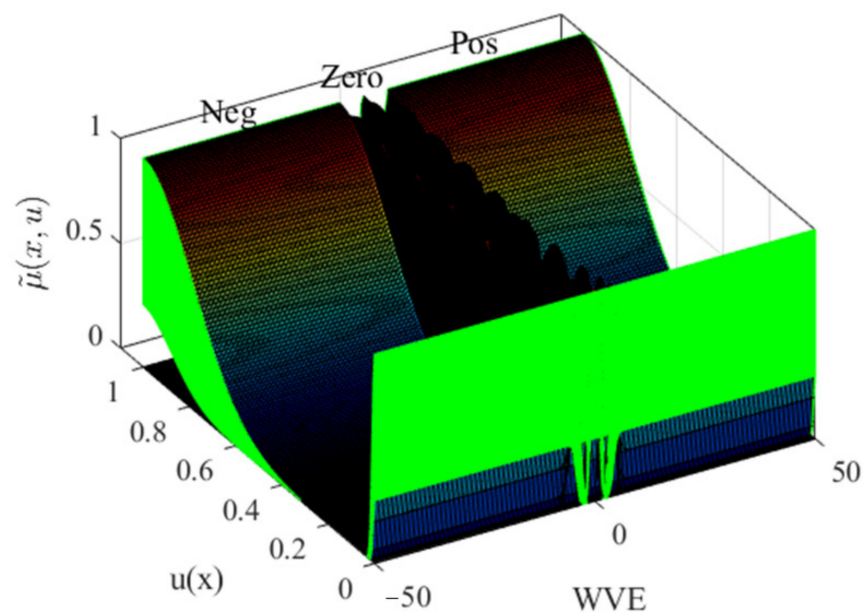


Figure 7. The architecture of the antecedent membership function (WVE).

The parameters for the construction of the antecedents are presented in Table 2.

Table 2. T3 MF antecedent parameters.

| | | | | | LVE | | |
|-------|-----|-----|-----|----|-----------|----------|----------|
| T3 MF | a1 | b1 | c1 | d1 | λ | ℓ_1 | ℓ_2 |
| Neg | -50 | -50 | -15 | -1 | 0.3 | 0.2 | 0.2 |
| Zero | -4 | 0 | 4 | - | 0.3 | 0.2 | 0.2 |
| Pos | 1 | 5 | 50 | 50 | 0.3 | 0.2 | 0.2 |
| | | | | | WVE | | |
| T3 MF | a1 | b1 | c1 | d1 | λ | ℓ_1 | ℓ_2 |
| Neg | -50 | -50 | -15 | -1 | 0.3 | 0.2 | 0.2 |
| Zero | -4 | 0 | 4 | - | 0.3 | 0.2 | 0.2 |
| Pos | 1 | 5 | 50 | 50 | 0.3 | 0.2 | 0.2 |

The rules for the IT3FC mobile robot system are presented in Table 3 and the parameters for the construction of the consequents are presented in Table 4. The consequents are made up of the parameters [C S], where C = Center and S = Spread (Uncertainty Ratio).

Table 3. Rules for the IT3FC mobile robot system.

| LVE | WVE | Torque 1 | Torque 2 |
|------|------|----------|----------|
| Neg | Neg | -50 | -50 |
| Neg | Zero | -50 | 0 |
| Neg | Pos | -50 | 50 |
| Zero | Neg | 0 | -50 |
| Zero | Zero | 0 | 0 |
| Zero | Pos | 0 | 50 |
| Pos | Neg | 50 | -50 |
| Pos | Zero | 50 | 0 |
| Pos | Pos | 50 | 50 |

Table 4. Consequents parameters.

| | | C | | | S |
|----------|--|-----|------|-----|----|
| | | Neg | Zero | Pos | |
| Torque 1 | | -50 | 0 | 50 | 10 |
| Torque 2 | | -50 | 0 | 50 | 10 |

The surface generated to control the right (Torque 1) and left (Torque 2) wheels can be seen in Figures 8 and 9, respectively.

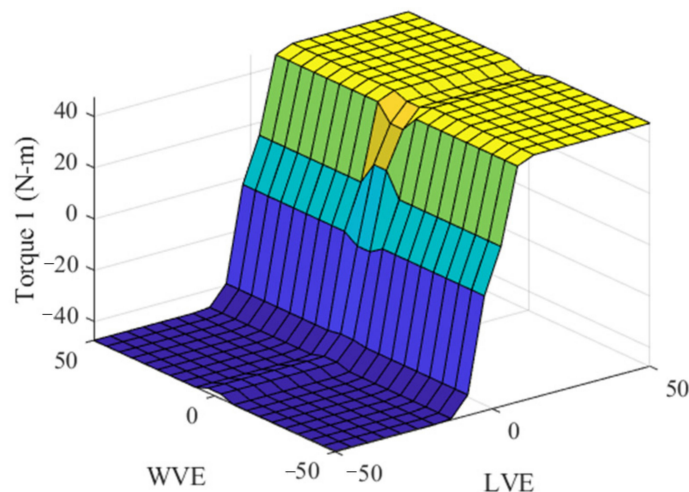


Figure 8. Torque 1 surface.

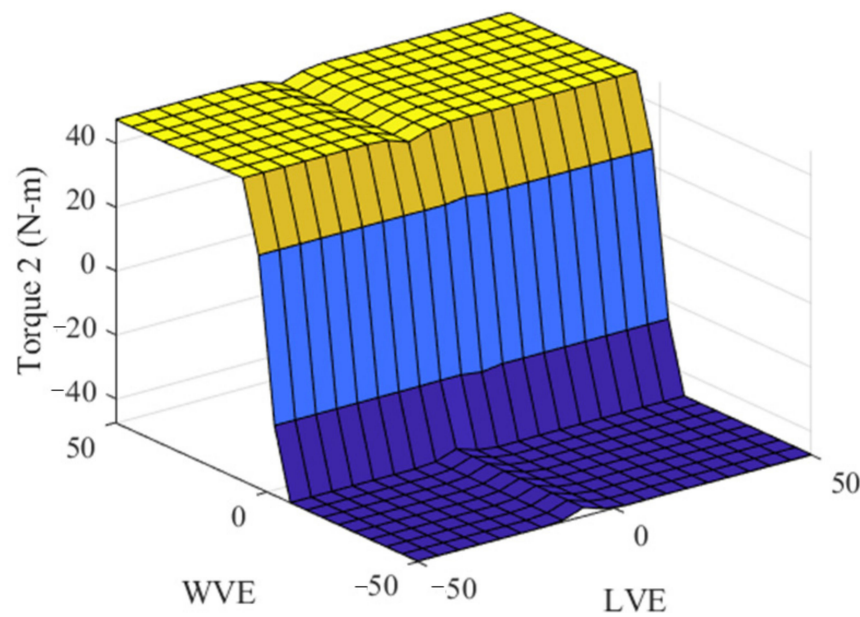


Figure 9. Torque 2 surface.

5. Results

IT3FDE was in charge of adjusting the parameter F during the generations and finding the best parameterization of the T3 MF of the mobile robot system. In total, 10 parameters were optimized.

Different simulations were performed, the controller was optimized without noise and three different noise levels were applied: The first is band-limited white noise (BLW), the second is pulse generated noise (PG) and the third is uniform random number noise (URN). The parameter values applied to each noise level were as follows: for the BLW, the height of the Power Spectral Density was managed at 0.1; the values 1, 1, 5 and 0, were set for the amplitude, the period, pulse width (%) and phase, respectively, for the PG; finally, the amplitude of [-1,1] was set for the URN.

The parameters used for experimentation with noise and without noise are summarized in Table 5.

Table 5. IT3FDE parameter values.

| Parameter | Value |
|-------------|---------|
| F | Dynamic |
| CR | 0.5 |
| NP | 45 |
| Generations | 100 |
| Simulations | 30 |

The metrics used to measure the performance of the IT3FDE are shown in Equations (40)–(45).

$$ITAE = \sum_{t=1}^N t (x(t) - \hat{x}(t)) \tag{40}$$

$$ITSE = \sum_{t=1}^N t \left((x(t) - \hat{x}(t))^2 \right) \tag{41}$$

$$IAE = \sum_{t=1}^N |x(t) - \hat{x}(t)| \tag{42}$$

$$ISE = \sum_{t=1}^N |(x(t) - \hat{x}(t))^2| \tag{43}$$

$$RMSE = \sqrt{\frac{1}{N} \sum_{t=1}^N (x_t - \hat{x}_t)^2} \tag{44}$$

$$MSE = \frac{1}{n} \sum_{i=1}^n (\bar{Y}_i - Y_i)^2 \tag{45}$$

Table 6 presents the obtained simulations without applying noise to the controller.

Table 6. Metrics results without noise.

| Metrics | LVE | WVE |
|----------------|------------------------|------------------------|
| | IT3FC | IT3FC |
| ITAE | 7.06×10^1 | 4.90×10^1 |
| ITSE | 1.07×10^1 | 2.33×10^0 |
| IAE | 2.99×10^0 | 2.00×10^0 |
| ISE | 6.70×10^{-01} | 1.00×10^{-01} |
| RMSE | 2.68×10^0 | 4.00×10^{-03} |
| MSE | 1.64×10^0 | 6.60×10^{-02} |
| Execution time | 22,051.8 s | |

Table 6 shows the most used performance indices in control systems to determine if the controller parameters were optimally obtained, we can observe the ITAE, ITSE, IAE and ISE errors, the latter is considered an optimal value because its value is minimized, this tells us we will have a smooth weight because the error shown is small. The errors obtained from the RMSE and MSE are presented, the aim is to minimize the error for more excellent controller stability. Finally, the execution time of the 30 experiments carried out without applying noise to the controller is presented.

Table 7 shows the errors and the time obtained from the experimentation with the proposed method when applying three different noise levels. When analyzing these results, it can be determined that the controller achieves stability because in the three types of noise presented, the ISE, RMSE and MSE error decrease considerably. It can be seen that when using URN noise, the results are better compared to the other noise levels presented for this case study.

Table 7. Simulations obtained applying the BLW, PG, URN, respectively.

| Metrics | BLW | | PG | | URN | |
|----------------|--------------------|------------------------|--------------------|------------------------|------------------------|------------------------|
| | LVE IT3FC | WVE IT3FC | LVE IT3FC | WVE IT3FC | LVE IT3FC | WVE IT3FC |
| ITAE | 8.01×10^2 | 7.72×10^2 | 9.75×10^1 | 4.03×10^1 | 7.18×10^1 | 5.02×10^1 |
| ITSE | 8.13×10^2 | 7.68×10^2 | 1.77×10^1 | 2.05×10^0 | 1.07×10^1 | 2.40×10^0 |
| IAE | 3.25×10^1 | 3.13×10^1 | 4.07×10^0 | 1.79×10^0 | 3.05×10^0 | 2.03×10^0 |
| ISE | 3.34×10^1 | 3.17×10^1 | 1.06×10^0 | 1.70×10^{-01} | 6.70×10^{-01} | 1.00×10^{-01} |
| RMSE | 3.65×10^0 | 3.30×10^{-01} | 3.69×10^0 | 4.40×10^{-01} | 2.69×10^0 | 1.00×10^{-02} |
| MSE | 1.91×10^0 | 5.70×10^{-01} | 1.92×10^0 | 6.70×10^{-01} | 1.64×10^0 | 7.00×10^{-02} |
| Execution time | 25,519.5 s | | 26,237.9 s | | 27,075.5 s | |

Tables 8–10 show the comparison with other existing methods in the literature [37], a comparison is made using the different types of noise mentioned above as well as the different types of controllers type-1(T1FC), interval type-2, (IT2FC) generalized type 2 (GT2FC) and finally, an interval type-3 (IT3FC).

Table 8. Metrics results with BLW.

| Metrics | LVE | | | |
|---------|--------------------|--------------------|--------------------|--------------------|
| | T1FC | IT2FC | GT2FC | IT3FC |
| ITAE | 1.35×10^2 | 1.20×10^2 | 1.17×10^2 | 8.01×10^2 |
| ITSE | 1.44×10^2 | 1.10×10^2 | 1.04×10^2 | 8.13×10^2 |
| IAE | 1.37×10^1 | 1.22×10^1 | 1.18×10^1 | 3.25×10^1 |
| ISE | 1.50×10^1 | 1.13×10^1 | 1.06×10^1 | 3.34×10^1 |
| WVE | | | | |
| ITAE | 1.37×10^2 | 1.20×10^2 | 1.14×10^2 | 7.72×10^2 |
| ITSE | 1.53×10^2 | 1.11×10^2 | 1.01×10^2 | 7.68×10^2 |
| IAE | 1.40×10^1 | 1.22×10^1 | 1.17×10^1 | 3.13×10^1 |
| ISE | 1.60×10^1 | 1.16×10^1 | 1.06×10^1 | 3.17×10^1 |

Table 9. Metrics results with PG.

| Metrics | LVE | | | |
|---------|------------------------|------------------------|------------------------|------------------------|
| | T1FC | IT2FC | GT2FC | IT3FC |
| ITAE | 2.74×10^1 | 2.64×10^1 | 2.42×10^1 | 9.75×10^1 |
| ITSE | 9.44×10^0 | 7.07×10^0 | 5.27×10^0 | 1.77×10^1 |
| IAE | 2.90×10^0 | 2.95×10^0 | 2.74×10^0 | 4.07×10^0 |
| ISE | 1.12×10^0 | 1.11×10^0 | 9.10×10^{-01} | 1.06×10^0 |
| WVE | | | | |
| ITAE | 1.81×10^1 | 1.57×10^1 | 1.32×10^1 | 4.03×10^1 |
| ITSE | 7.14×10^0 | 3.70×10^0 | 2.26×10^0 | 2.05×10^0 |
| IAE | 2.17×10^0 | 2.15×10^0 | 1.90×10^0 | 1.79×10^0 |
| ISE | 9.90×10^{-01} | 9.40×10^{-01} | 7.90×10^{-01} | 1.70×10^{-01} |

Table 10. Metric results with URN.

| Metric | LVE | | | |
|--------|--------------------|--------------------|--------------------|------------------------|
| | T1FC | IT2FC | GT2FC | IT3FC |
| ITAE | 8.01×10^1 | 6.47×10^1 | 5.94×10^1 | 7.18×10^1 |
| ITSE | 5.17×10^1 | 3.30×10^1 | 2.84×10^1 | 1.07×10^1 |
| IAE | 8.52×10^0 | 7.10×10^0 | 6.56×10^0 | 3.05×10^0 |
| ISE | 5.80×10^0 | 4.22×10^0 | 3.69×10^0 | 6.70×10^{-01} |
| WVE | | | | |
| ITAE | 8.19×10^1 | 6.52×10^1 | 5.99×10^1 | 5.02×10^1 |
| ITSE | 5.14×10^1 | 3.14×10^1 | 2.67×10^1 | 2.40×10^0 |
| IAE | 8.67×10^0 | 7.17×10^0 | 6.67×10^0 | 2.03×10^0 |
| ISE | 5.83×10^0 | 4.10×10^0 | 3.63×10^0 | 1.00×10^{-01} |

The comparison of the different controllers using the BLW noise shows that there is no difference between the results, they are all in the same order. Although we can see that IT3FC does not have a better performance, it is considered competitive with respect to others.

Table 9 shows a comparison of the different errors using a PG noise. In this case, we can see that in the case of LVE the GT2FC has a better performance than IT3FC but nevertheless, the difference between the two is not considerable. On the other hand, from the comparison with the WVE, we can see that IT3FC has a better result than GT2FC, even though they have an error of the same order.

The last noise used is URN and for this comparison, it is observed that both in LVE and WVE, the proposal used IT3FC is better for both cases compared to T1FC, IT2FC and GT2FC.

Figures 10–13 show the best and worst simulation obtained with the IT3FC by optimizing the parameters with the IT3FDE proposed method, without noise, with BLW noise, with PG noise, and finally with URN noise, respectively.

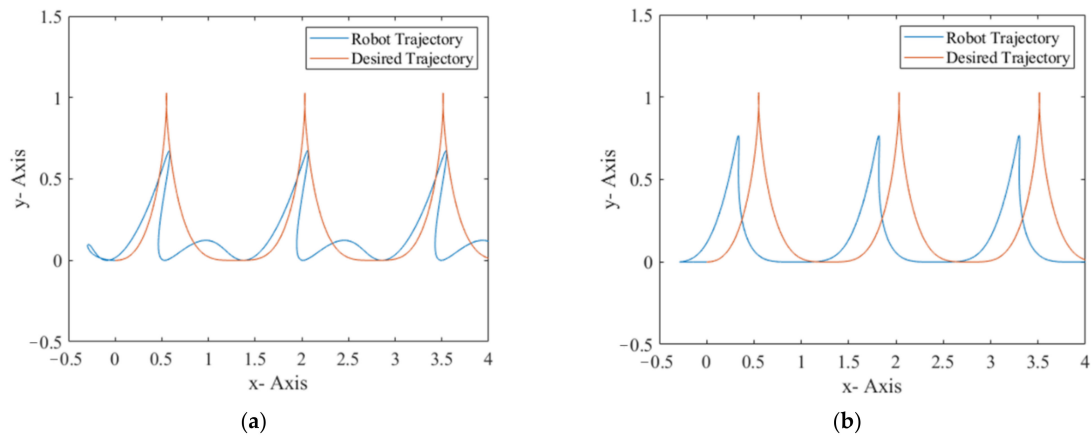


Figure 10. Comparison of (a) best simulation with the IT3FC and (b) worst simulation with the IT3FC proposed methods without noise.

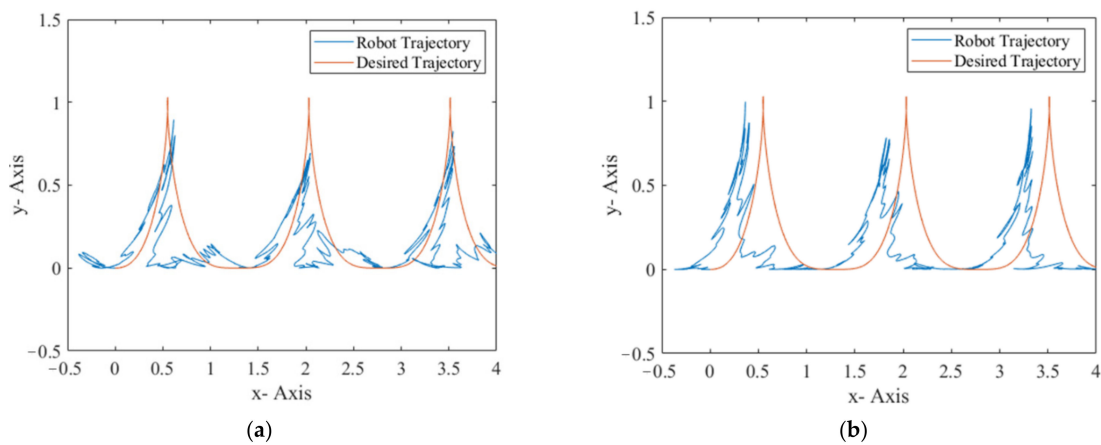


Figure 11. Comparison of (a) best simulation with the IT3FC and (b) worst simulation with the IT3FC proposed methods with BLW noise.

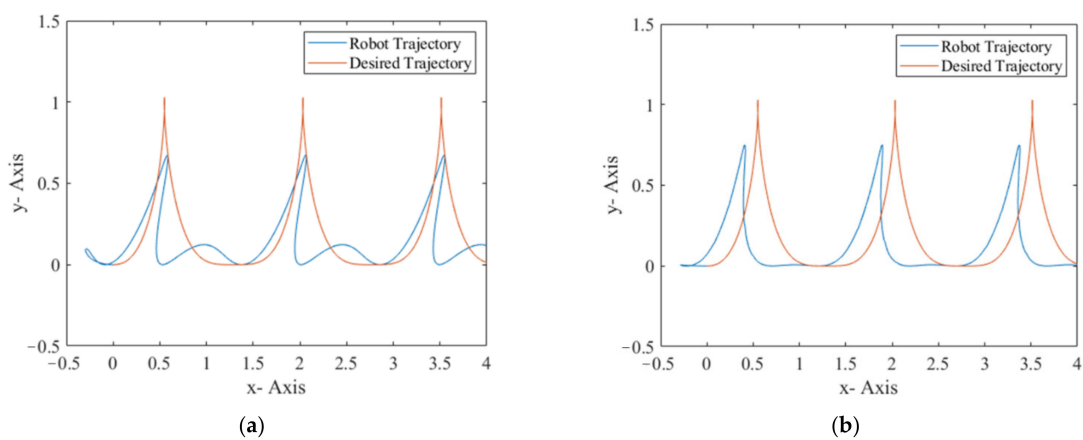


Figure 12. Comparison of (a) best simulation with the IT3FC and (b) worst simulation with the IT3FC proposed methods with PG noise.

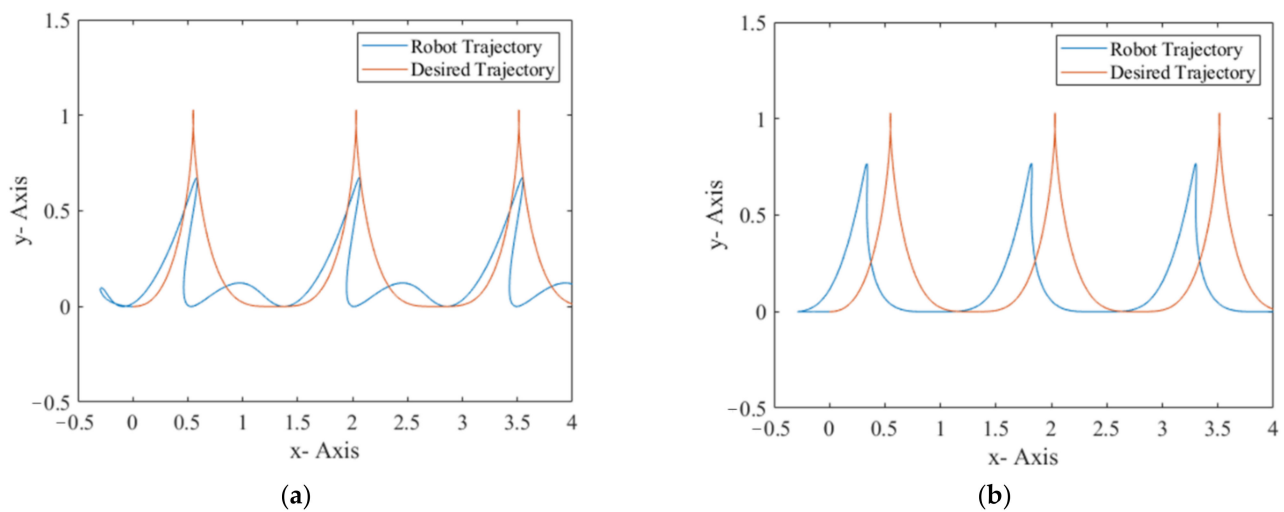


Figure 13. Comparison of (a) best simulation with the IT3FC and (b) worst simulation with the IT3FC proposed method with URN noise.

6. Conclusions

The main contribution was the implementation of a novel parameter adaptation approach for the DE algorithm proposed by utilizing the parameterization of interval type-3 membership functions using vertical cuts with the goal of managing in a better fashion the uncertainty of the parameter setting problem in the DE algorithm and the implementation of the parameterization of interval type-3 membership functions using vertical cuts in a Sugeno IT3-FSs for controlling a mobile robot.

The implementation of a Sugeno IT3-FSs controller is novel, as there are mostly Sugeno controllers that use type-1 and type-2.

Six different metrics were used to check the effectiveness of the method and compare them with previous work in the literature; the results obtained with the controller without applying any type of disturbance in the controller are competitive compared to the results presented in another article in the literature with a white noise level.

The errors of the controller linear and angular errors are compared against the results of existing articles in the literature. It can be seen that the error obtained by IT3FC when applying white noise is higher compared to the other methods, (T1FC, IT2FC, GT2FC). Analyzing the results when applying pulse generated noise, the ITSE, IAE and ISE errors are similar in the different controller types. The best results were found when using the noise uniform random number.

With the comparisons made, it can be seen that the use of interval type-3 fuzzy system implemented in a controller presents an improvement when uncertainty is added. This controller uses a lower scale of 0.3, therefore the uncertainty of 0.7 was used in the controller.

In the analysis of the results presented in this article, the objective of stabilizing the controller is achieved by obtaining a minimum value in the ISE metric in the implementations carried out with the parameterization of interval type-3 membership functions using the vertical cuts proposed methodology and is demonstrated that this methodology can be competing against others existing in the literature.

Author Contributions: Development on the specific topic as well as revisions in the literature in order to create the main contribution as well as capture the idea and writing C.P., P.O. and O.C.; Supervision, O.C. and Z.W.G. All authors have read and agreed to the published version of the manuscript.

Funding: This research received no external funding.

Data Availability Statement: Not applicable.

Acknowledgments: We thank Tijuana Institute of Technology, TecNM and UABC University.

Conflicts of Interest: The authors declare no conflict of interest.

References

1. Houssein, E.H.; Abohashima, Z.; Elhoseny, M.; Mohamed, W.M. Machine learning in the quantum realm: The state-of-the-art, challenges, and future vision. *Expert Syst. Appl.* **2022**, *194*, 116512. [[CrossRef](#)]
2. Mittal, K.; Jain, A.; Vaisla, K.S.; Castillo, O.; Kacprzyk, J.A. comprehensive review on type 2 fuzzy logic applications: Past, present and future. *Eng. Appl. Artif. Intell.* **2020**, *95*, 103916. [[CrossRef](#)]
3. Cao, Y.; Raise, A.; Mohammadzadeh, A.; Rathinasamy, S.; Band, S.S.; Mosavi, A. Deep learned recurrent type-3 fuzzy system: Application for renewable energy modeling/prediction. *Energy Rep.* **2021**, *7*, 8115–8127. [[CrossRef](#)]
4. Zhan, Z.-H.; Li, J.-Y.; Zhang, J. Evolutionary deep learning: A survey. *Neurocomputing* **2022**, *483*, 42–58. [[CrossRef](#)]
5. Zadeh, L.A. Fuzzy Sets. *Information and Control.* **1965**, *8*, 338–353. [[CrossRef](#)]
6. Zhou, X.; Ma, H.; Gu, J.; Chen, H.; Deng, W. Parameter adaptation-based ant colony optimization with dynamic hybrid mechanism. *Eng. Appl. Artif. Intell.* **2022**, *114*, 105139. [[CrossRef](#)]
7. Melin, P.; Miramontes, I.; Carvajal, O.; Prado-Arechiga, G. Fuzzy dynamic parameter adaptation in the bird swarm algorithm for neural network optimization. *Soft Comput.* **2022**, *26*, 9497–9514. [[CrossRef](#)]
8. Cuevas, F.; Castillo, O.; Cortes, P. Optimal Setting of Membership Functions for Interval Type-2 Fuzzy Tracking Controllers Using a Shark Smell Metaheuristic Algorithm. *Int. J. Fuzzy Syst.* **2022**, *24*, 799–822. [[CrossRef](#)]
9. Guerrero, M.; Valdez, F.; Castillo, O. A New Cuckoo Search Algorithm Using Interval Type-2 Fuzzy Logic for Dynamic Parameter Adaptation. In *International Conference on Intelligent and Fuzzy Systems*; Springer: Cham, Switzerland, 2021; pp. 853–860.
10. Kahraman, C.; Cebi, S.; Cevik Onar, S.; Oztaysi, B.; Tolga, A.C.; Sari, I.U. Intelligent and Fuzzy Techniques for Emerging Conditions and Digital Transformation. *Springer Int. Publ.* **2022**, *308*, 853–860.
11. Cuevas, F.; Castillo, O.; Cortés-Antonio, P. Generalized Type-2 Fuzzy Parameter Adaptation in the Marine Predator Algorithm for Fuzzy Controller Parameterization in Mobile Robots. *Symmetry* **2022**, *14*, 859. [[CrossRef](#)]
12. Carvajal, O.; Melin, P.; Miramontes, I.; Prado-Arechiga, G. Optimal design of a general type-2 fuzzy classifier for the pulse level and its hardware implementation. *Eng. Appl. Artif. Intell.* **2021**, *97*, 104069. [[CrossRef](#)]
13. Ochoa, P.; Castillo, O.; Melin, P.; Soria, J. Differential Evolution with Shadowed and General Type-2 Fuzzy Systems for Dynamic Parameter Adaptation in Optimal Design of Fuzzy Controllers. *Axioms* **2021**, *10*, 194. [[CrossRef](#)]
14. Castillo, O.; Peraza, C.; Ochoa, P.; Amador-Angulo, L.; Melin, P.; Park, Y.; Geem, Z.W. Shadowed Type-2 Fuzzy Systems for Dynamic Parameter Adaptation in Harmony Search and Differential Evolution for Optimal Design of Fuzzy Controllers. *Mathematics* **2021**, *9*, 2439. [[CrossRef](#)]
15. Ahmadini, A.A.H. A novel technique for parameter estimation in intuitionistic fuzzy logistic regression model. *Ain Shams Eng. J.* **2022**, *13*, 101518. [[CrossRef](#)]
16. Yolcu, O.C.; Egrioglu, E.; Bas, E.; Yolcu, U. Multivariate intuitionistic fuzzy inference system for stock market prediction: The cases of Istanbul and Taiwan. *Appl. Soft Comput.* **2022**, *116*, 108363. [[CrossRef](#)]
17. Castillo, O.; Castro, J.R.; Melin, P. A methodology for building interval type-3 fuzzy systems based on the principle of justifiable granularity. *Int. J. Intell. Syst.* **2022**, *37*, 7909–7943. [[CrossRef](#)]
18. Liu, Z.; Mohammadzadeh, A.; Turabieh, H.; Mafarja, M.; Band, S.S.; Mosavi, A. A new online-learned interval type-3 fuzzy control system for solar energy management systems. *IEEE Access* **2021**, *9*, 10498–10508. [[CrossRef](#)]
19. Castillo, O.; Pulido, M.; Melin, P. Interval Type-3 Fuzzy Aggregators for Ensembles of Neural Networks in Time Series Prediction. *Int. Conf. Intell. Fuzzy Syst.* **2022**, *114*, 785–793.
20. Tian, M.W.; Yan, S.R.; Mohammadzadeh, A.; Tavoosi, J.; Mobayen, S.; Safdar, R.; Zhilenkov, A. Stability of Interval Type-3 Fuzzy Controllers for Autonomous Vehicles. *Mathematics* **2021**, *9*, 2742. [[CrossRef](#)]
21. Mohammadzadeh, A.; Castillo, O.; Band, S.S.; Mosavi, A. A novel fractional-order multiple-model type-3 fuzzy control for nonlinear systems with unmodeled dynamics. *Int. J. Fuzzy Syst.* **2021**, *23*, 1633–1651. [[CrossRef](#)]
22. Aly, A.A.; Felemban, B.F.; Mohammadzadeh, A.; Castillo, O.; Bartoszewicz, A. Frequency Regulation System: A Deep Learning Identification, Type-3 Fuzzy Control and LMI Stability Analysis. *Energies* **2021**, *14*, 7801. [[CrossRef](#)]
23. Alattas, K.A.; Mohammadzadeh, A.; Mobayen, S.; Aly, A.A.; Felemban, B.F.; Vu, M.T. A New Data-Driven Control System for MEMS Gyroscopes: Dynamics Estimation by Type-3 Fuzzy Systems. *Micromachines* **2021**, *12*, 1390. [[CrossRef](#)] [[PubMed](#)]
24. Castillo, O.; Castro, J.R.; Melin, P. Interval Type-3 Fuzzy Control for Automated Tuning of Image Quality in Televisions. *Axioms* **2022**, *11*, 276. [[CrossRef](#)]
25. Castillo, O.; Castro, J.R.; Melin, P. Introduction to Interval Type-3 Fuzzy Systems. In *Interval Type-3 Fuzzy Systems: Theory and Design*; Springer: Berlin/Heidelberg, Germany, 2022; pp. 1–4.
26. Abdelkader, E.M.; Moselhi, O.; Marzouk, M.; Zayed, T. An exponential chaotic differential evolution algorithm for optimizing bridge maintenance plans. *Autom. Constr.* **2022**, *134*, 104107. [[CrossRef](#)]
27. Kharchouf, Y.; Herbazi, R.; Chahboun, A. Parameter's extraction of solar photovoltaic models using an improved differential evolution algorithm. *Energy Convers. Manag.* **2022**, *251*, 114972. [[CrossRef](#)]
28. DE Athayde Prata, B.; Rodrigues, C.D.; Framinan, J.M. A differential evolution algorithm for the customer order-scheduling problem with sequence-dependent setup times. *Expert Syst. Appl.* **2022**, *189*, 116097. [[CrossRef](#)]

29. Peng, Y.; He, S.; Sun, K. Parameter identification for discrete memristive chaotic map using adaptive differential evolution algorithm. *Nonlinear Dyn.* **2022**, *107*, 1263–1275. [[CrossRef](#)]
30. Wang, G.G.; Gao, D.; Pedrycz, W. Solving multi-objective fuzzy job-shop scheduling problem by a hybrid adaptive differential evolution algorithm. *IEEE Trans. Ind. Inform.* **2022**, *early access*. [[CrossRef](#)]
31. Dash, S.K.; Mishra, S.; Abdelaziz, A.Y.; Alghaythi, M.L.; Allehyani, A. Optimal Allocation of Distributed Generators in Active Distribution Networks Using a New Oppositional Hybrid Sine Cosine Muted Differential Evolution Algorithm. *Energies* **2022**, *15*, 2267. [[CrossRef](#)]
32. He, Y.; Zhang, F.; Mirjalili, S.; Zhang, T. Novel binary differential evolution algorithm based on Taper-shaped transfer functions for binary optimization problems. *Swarm Evol. Comput.* **2022**, *69*, 101022. [[CrossRef](#)]
33. Castillo, O.; Valdez, F.; Soria, J.; Yoon, J.H.; Geem, Z.W.; Peraza, C.; Ochoa, P.; Amador-Angulo, L. Optimal Design of Fuzzy Systems Using Differential Evolution and Harmony Search Algorithms with Dynamic Parameter Adaptation. *Appl. Sci.* **2020**, *10*, 6146. [[CrossRef](#)]
34. Peraza, C.; Valdez, F.; Melin, P. Optimization of Intelligent Controllers Using a Type-1 and Interval Type-2 Fuzzy Harmony Search Algorithm. *Algorithms* **2017**, *10*, 82. [[CrossRef](#)]
35. Ochoa, P.; Castillo, O.; Soria, J. Optimization of fuzzy controller design using a Differential Evolution algorithm with dynamic parameter adaptation based on Type-1 and Interval Type-2 fuzzy systems. *Soft Comput.* **2020**, *24*, 193–214. [[CrossRef](#)]
36. Bernal, E.; Lagunes, M.L.; Castillo, O.; Soria, J.; Valdez, F. Optimization of Type-2 Fuzzy Logic Controller Design Using the GSO and FA Algorithms. *Int. J. Fuzzy Syst.* **2021**, *23*, 42–57. [[CrossRef](#)]
37. Sanchez, M.A.; Castillo, O.; Castro, J.R. Generalized Type-2 Fuzzy Systems for controlling a mobile robot and a performance comparison with Interval Type-2 and Type-1 Fuzzy Systems. *Expert Syst. Appl.* **2015**, *42*, 5904–5914. [[CrossRef](#)]